states, resulting in more facile cleavage of this bond. Our conclusion is that CAD spectra of small oligosaccharides may be rich in information on position of linkage and perhaps other stereochemical parameters due to these internal, nonbonding interactions. We are currently studying other series of synthetic saccharides, with differences in position of linkage, anomeric configuration, and with amino and neutral sugars.

Therefore, this is the first systematic MS-CAD-MS and molecular modeling study of a heterooligosaccharide series that clearly shows linkage position in the intact, underivatized compound. FABMS-CAD, in combination with the predictive value for fragmentation using computed motional freedom, shows promise for MS-CAD-MS for precisely fingerprinting oligosaccharide structures based on their internal nonbonding steric energies using calculation of conformational density of states at the transition-state energy corresponding to bond scission.

Registry No. F3, 115921-23-8; F4, 116079-23-3; F6, 116148-08-4.

Adsorption and Decomposition of Dimethyl Methylphosphonate on Platinum(111)

M. A. Henderson and J. M. White*

Contribution from the Department of Chemistry, University of Texas, Austin, Texas 78712.
Received March 16, 1988

Abstract: The interaction of dimethyl methylphosphonate (DMMP) with Pt(111) was studied with high-resolution electron energy loss spectroscopy (HREELS), positive and negative static secondary ion mass spectrometry (SSIMS), temperature-programmed desorption (TPD), and Auger electron spectroscopy (AES). DMMP, a common simulant of more toxic organophosphonate esters, binds strongly and molecularly to Pt(111) at 100 K. HREEL results indicate that it binds through the oxygen lone pairs on the -P=O. Decomposition occurs after heating above 300 K, yielding exclusively CO and H_2 in TPD, with P and a small amount of C left on the surface. The decomposition mechanism first involves PO-CH_3 bond cleavage (300-400 K), with some P-OCH_3 cleavage at high-DMMP coverages, and then P-CH_3 bond cleavage (400-500 K), leaving predominantly PO and an unidentified PO_x species. Both species are stable to at least 500 K. The catalytic applicability of Pt for decomposition of organophosphorus compounds in a nonoxidizing environment is limited by the accumulation of surface P.

1. Introduction

The catalytic decomposition of organophosphorus compounds is of great importance for health and environmental safety.[1] Although these compounds have agricultural, industrial, and military applications, little is known about their molecular chemistry on clean metal and oxide surfaces. Understanding of how organophosphorus compounds interact with these surfaces can lead to better systems for their catalytic decomposition. This paper is a continuation of our work on the interaction of phosphorus-containing molecules with metal and oxide surfaces.[2-9]

Dimethyl methylphosphonate (DMMP), $O{=}P(CH_3)(OCH_3)_2$, is often used to simulate the chemical and structural properties of more toxic organophosphorus compounds.[1] Previous DMMP-substrate research has involved Rh(100),[4] Mo(110),[10] Pt wire,[11] oxidized Fe,[3] Pt/Al_2O_3,[12] Al_2O_3,[13] SiO_2, and Fe_2O_3.[8] These works have been summarized elsewhere,[10] and we focus on those of particular imporance to this study. Graven and co-workers observed catalytic oxidation of DMMP when a DMMP-air or DMMP-N_2 mixture was passed over a commercial alumina-supported Pt catalyst held between 573 and 773 K. The major decomposition products in air were CH_3OH and CO_2, but no CO_2 was observed in the N_2 flow. Catalyst deactivation occurred below reactor temperatures of 720 K; however, a 100% conversion rate was maintained at 770 K. A detailed inelastic electron-tunneling spectroscopy (IETS) study by Templeton and Weinberg[13] has shown that DMMP decomposes on Al_2O_3 in steps according to

$$\text{DMMP} \xrightarrow{295\ \text{K}} \text{MMP} \xrightarrow{573\ \text{K}} \text{MP} \qquad (1)$$

where MMP = methyl methylphosphonate ($CH_3P(OCH_3)O_2$) and MP = methylphosphonate (CH_3PO_3) with CH_3OH emitted at each decomposition step. The P-CH_3 bond was stable to at least 673 K. The durability of the P-CH_3 bond may partially explain the catalytic deactivation observed by Graven et al. below 750 K. However, the role of the Pt in this process has not been determined.

Using laser-induced fluorescence (LIF), Dulcey et al.[11] observed the desorption of PO radicals, along with CH_4, H_2, and CO, when (2.5-7.3) × 10^{-5} Torr DMMP was passed over a Pt wire above

(1) Ekerdt, J. G.; Klabunde, K. J.; Shapley, J. R.; White, J. M.; Yates, J. T., Jr., submitted for publication in *J. Phys. Chem.*
(2) Hedge, R. I.; White, J. M. *J. Phys. Chem.* **1986**, *90*, 2159.
(3) Hegde, R. I.; White, J. M. *Appl. Surf. Sci.* **1987**, *28*, 1.
(4) Hegde, R. I.; Greenlief, C. M.; White, J. M. *J. Phys. Chem.* **1985**, *89*, 2886.
(5) Greenlief, C. M.; Hegde, R. I. White, J. M. *J. Phys. Chem.* **1985**, *89*, 5681.
(6) Mitchell, G. E.; Henderson, M. A.; White, J. M. *J. Phys. Chem.* **1987**, *91*, 3808.
(7) Mitchell, G. E.; Henderson, M. A.; White, J. M.; *Surf. Sci.* **1987**, *191*, 425.
(8) Henderson, M. A.; Jin, T.; White, J. M. *J. Phys. Chem.* **1986**, *90*, 4607.
(9) Hegde, R. I.; Tobin, J.; White, J. M. *J. Vac. Sci. Technol., A* **1985**, *3*, 339.
(10) Smentkowski, V. S.; Hagans, P.; Yates, J. T., Jr., submitted for publication in *J. Phys. Chem.*
(11) Dulcey, C. S.; Lin, M. C.; Hsu, C. C. *Chem. Phys. Lett.* **1985**, *115*, 481.
(12) Graven, W. M.; Weller, S. W.; Peters, D. L. I. & E. C. *Process Des. Dev.* **1966**, *5*, 1983.
(13) Templeton, M. K.; Weinberg, W. H. *J. Am. Chem. Soc.* **1985**, *107*, 97; *Ibid.* **1985**, *107*, 774.

0002-7863/88/1510-6939$01.50/0

1100 K. The production of PO was catalytic under these conditions, with an activation energy for desorption of 59 ± 2 kcal/mol. Catalyst deactivation was observed after long exposures, presumably due to P and C accumulation on the surface. Incorporation of 1×10^{-6} Torr O_2 into the flow system enhanced PO production but did not thwart catalytic deactivation.

While the work of Dulcey et al.[11] indicates that Pt has some application as a catalyst for organophosphorus decomposition, surface analysis was not involved. We focus on the structural and kinetic interactions of DMMP with Pt(111) by means of high-resolution electron energy loss spectroscopy (HREELS), static secondary ion mass spectrometry (SSIMS), temperature-programmed desorption (TPD), and Auger electron spectroscopy (AES). Our results indicate that DMMP decomposes on Pt(111) above 300 K first by PO–C and P–OC bond cleavage (300–450 K) and then by P–C and P–O bond cleavage (400–450 K), leaving PO, O, and CH as the major surface species. PO is stable to at least 500 K. TPD products of DMMP decomposition are CO and H_2, with P and a small amount of C left on the surface. The applicability of Pt for catalytic decomposition of organophosphorus compounds is discussed in light of these results.

2. Experimental Section

The ultrahigh-vacuum chamber used in this study and the methods of data collection have been detailed elsewhere.[14] The system is ion-pumped with a working base pressure of 1×10^{-10} Torr. The system's gas handling line was evacuated by a 170 L/s turbomolecular pump. The HREELS spectrometer is a 127° cylindrical sector type with stationary monochromator and analyzer defining a total scattering angle of 120°. All spectra were taken in the specular direction with a primary beam energy of 6.9 ± 0.3 eV and resolution of 10 mV full-width at half-maximum. SSIMS data were obtained with a primary Ar^+ energy of 1 keV and currents between 3 and 5 nA/cm^2. Ion detection was limited to the 0–120-amu region so we were unable to detect parent DMMP directly (124 amu).

Mounting, cooling, and heating of the Pt(111) crystal has also been described previously.[14] The temperature ramp rate for TPD and TPSSIMS experiments was 10 K/s. The sample was cleaned by Ar^+ bombardment and by oxidation at 800 K to remove carbon. The former was necessary to remove P left after DMMP thermal decomposition. Cleanliness was confirmed by AES and HREELS.

Commercial spectroscopic grade DMMP (Aldrich, 97% purity) was purified with several liquid N_2 freeze–pump–thaw cycles followed by continual pumping on the gas handling system in an ice–salt water bath (−14 °C). The latter treatment removed trace amounts of H_2O, CH_3OH, and methylphosphonic acid ($O{=}P(CH_3)(OH)_2$) impurities in DMMP. The latter two impurities result from hydrolysis of DMMP. Fresh samples of DMMP were prepared for each dose to minimize DMMP exposure to the walls of the gas handling system. DMMP was dosed through a directional doser consisting of a 0.2-cm-i.d. stainless steel tube connected by a leak valve to the gas handling system. (A second doser of this type delivered O_2 for surface cleaning.) During dosing, the sample face was perpendicular to the cylinder axis of the doser tube and was about 1 cm from its end. Exposures were based on the time spent in front of the doser at a DMMP flux that resulted in a 1×10^{-10} Torr pressure rise detected at the system's ion gauge (prior to rotating the sample in front of the doser). Actual exposures were not determined. The dosing temperature was 100 K.

3. Results

3.1. TPD. The TPD spectra of a 240-s DMMP exposure on Pt(111) at 100 K are shown in Figure 1. This exposure corresponds to many multilayers, thereby saturating the first layer and decomposition products resulting from it. In TPD the only decomposition products are CO and H_2. No CO_2, CH_3OH, CH_4, or phosphorus-containing compounds were detected. Small amounts of H_2O were occasionally detected at 190 K, especially after very large exposures. This is not due to decomposition of DMMP but to difficult-to-remove residual H_2O in the DMMP source. CO desorbs in three states at 437, 505, and 586 K. The former state resembles CO desorption from clean Pt(111), while the latter two are reaction limited. The peak at 212 K in Figure 1 is due to a DMMP reaction in the QMS (see below). H_2 desorbs

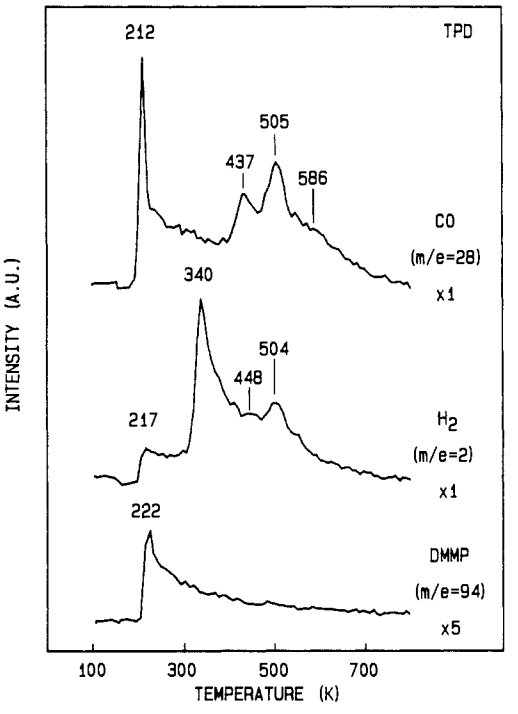

Figure 1. TPD of a 240-s DMMP exposure on Pt(111) at 100 K.

in at least two states at 340 and 504 K, with a possible third poorly resolved state at 448 K.

Comparison of the total yields of CO and H_2 with known saturation coverages of each on the clean surface (0.68 ML of CO[15] and 1.0 ML of H[6]) indicates that about 0.79 ML of H and 0.27 ML of CO desorb from DMMP decomposition (1 ML = 1 species/surface Pt atom). These values are nearly stoichiometric (3 H: 1 CO) and correspond to about 0.09 mL of DMMP decomposition on Pt(111). Because the first layer was saturated, we take these as maximum values. AES analysis after DMMP decomposition indicates that P and a small amount of C (<0.05 mL), but no O, are left on the surface. Stoichiometric quantification of P was not successful because of diffusion into the bulk during TPD.[6,7] Mild oxidation (1×10^{-8} Torr O_2 at 800 K) increased the P(120) to Pt(238) AES ratio by returning the P to the surface but did not remove P.

TPD following the m/e 94 ion ($PO_3CH_3^+$[10] and/or ($CH_3P(OH)(OCH_3)^+$[16]), one of the major cracking fragments of the parent, shows multilayer desorption at 222 K, but no discernible first-layer desorption state. Because our QMS ion source is not line-of-sight and DMMP adsorbs and/or decomposes readily on hot surfaces, molecular DMMP was detected only when relatively thick multilayers were adsorbed. The coincident CO and H_2 states at about 215 K are from displacement reactions within the SSIMS Bessel box that involve molecular DMMP desorption. A similar effect was observed for $P(CH_3)_3$ desorption from Pt(111).[6] Because these processes involve the adsorption of DMMP at the walls, molecular desorption from the first layer may go undetected.

Figure 2 shows the TPD of a low coverage of DMMP prepared by a 1-s DMMP exposure. Molecular DMMP was not detected, and there was no low-temperature 28-amu signal. We conclude that all of the DMMP decomposed. The amounts of CO (0.11 ML) and H_2 (0.32 ML of H) desorbed are again nearly stoichiometric and indicate that 0.035 ML of DMMP decomposed (about 40% of that in Figure 1). The major difference between the TPD of the two DMMP exposures is that the 437 K CO peak is absent in Figure 2. The peak positions and relative intensities of all the other H_2 and CO peaks are similar to the saturation coverage. Although 40% of the saturation decomposition was achieved after a 1-s dose, full saturation of decomposition required 120 s (not shown). This indicates that even though the sticking

(14) Mitchell, G. E.; Radloff, P. L.; Greenlief, C. M.; Henderson, M. A.; White, J. M. *Surf. Sci.* **1987**, *183*, 403.

(15) Ertl, G.; Neumann, M.; Streit, K. M. *Surf. Sci.* **1977**, *64*, 393.

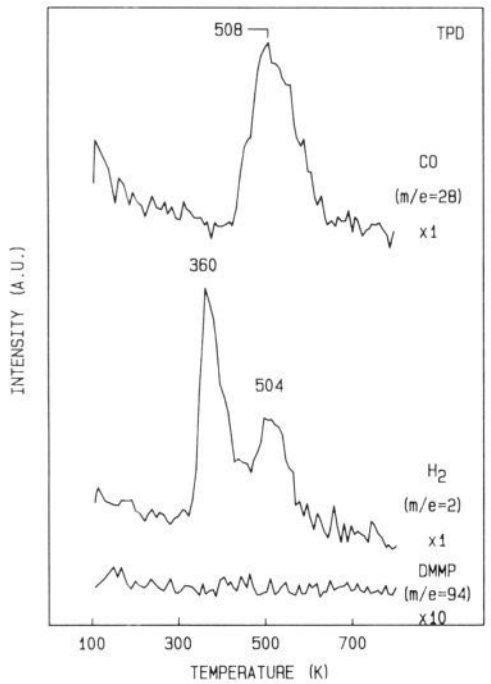

Figure 2. TPD of a 1-s DMMP exposure on Pt(111) at 100 K.

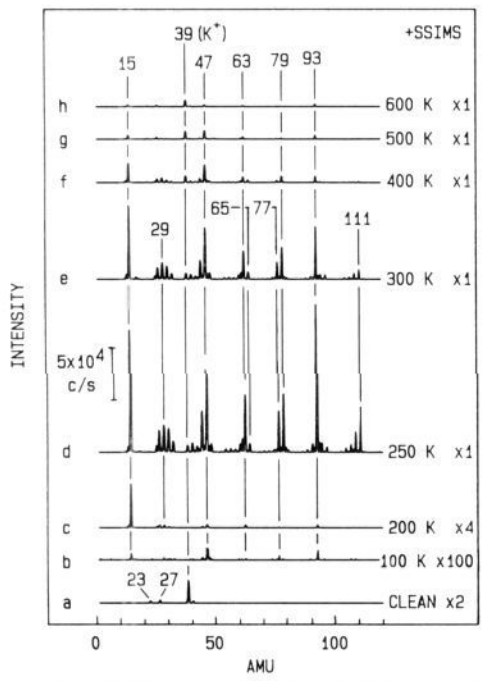

Figure 3. Positive SSIM spectra of (a) clean Pt(111) at 100 K and of a 600-s DMMP exposure on Pt(111) (b) at 100 K, followed by heating to (c) 200 K, (d) 250 K, (e) 300 K, (f) 400 K, (g) 500 K, and (h) 600 K.

coefficient is probably unity, completion of the first monolayer is incomplete when second-layer adsorption begins. Because of its relatively large size, fitting together a complete first layer of DMMP is difficult. We assume that when the decompositon saturates, the first layer of adsorbed DMMP is saturated.

3.2. SSIMS. Figures 3 and 4 show the positive and negative SSIM spectra (0–120 amu), respectively, at various annealing temperatures for a 600-s DMMP exposure on Pt(111). The major impurities on the clean surface (Figures 3a and 4a) are typical and include K^+ (m/e 39), Al^+ (m/e 27), Na^+ (m/e 23), O^- (m/e 16), and F^- (m/e 19). With the exception of O^-, these ions are absent from the SSIM spectra of a 600-s exposure of DMMP,

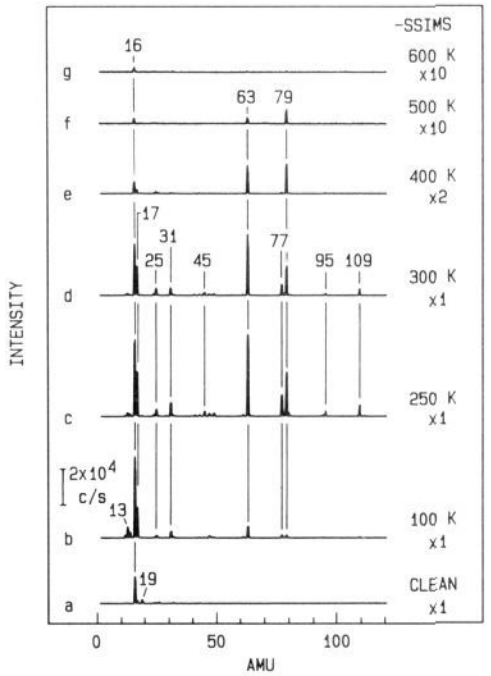

Figure 4. Negative SSIM spectra of (a) clean Pt(111) at 100 K and of a 600-s DMMP exposure on Pt(111) (b) at 100 K, followed by heating to (c) 250 K, (d) 300 K, (e) 400 K, (f) 500 K, and (g) 600 K.

Chart I

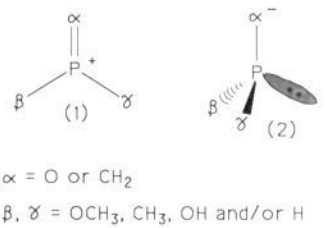

verifying that a thick multilayer covers the surface so that no SIMS ions come from the metal surface. At 100 K, SSIMS ion yields, particularly positive ions, from multilayer DMMP are low. The dominant ions are O^- and OH^- (m/e 17), with much smaller signals from $OP(OCH_3)CH_3^+$ (m/e 93), PO^+ (m/e 47), CH_3^+ (m/e 15), PO_3^- (m/e 79, $CH_2P(H)OCH_3^-$ (m/e 77), $OP(H)CH_3^-$ (m/e 63), PO_2^- (m/e 63), OCH_3^- (m/e 31), and CH_x^- (x = 0–2, m/e 12–14). Identificaton of the SSIMS ions was difficult since isotopically labeled DMMP was not available. However, a majority of P-containing ions fit the structures in Chart I, where α is O or CH_2 and β and γ are OCH_3, CH_3, OH, or H. The positive-ion structure (**1**) is common to the mass spectrum of DMMP[16,17] where α is predominantly O. Unlike what we observe by −SSIMS, the major negative ions in the gas-phase mass spectrum of DMMP are $(DMMP)H^-$ (m/e 125), $[OP(CH_3)(OCH_3)]H^-$ (m/e 92), and PCH_3^- (m/e 46).[16] Negative-ion mass spectra of several phosphotriesters are dominated by PO_3^- and PO_2^-.[18]

The negative-ion yields do not change significantly between 100 and 200 K; however, several of the positive ions, particularly $OP(OCH_3)CH_3^+$ (m/e 93), $PO_2^+/OP(H)CH_3^+$ (m/e 63), PO^+ (m/e 47), and CH_3^+ (m/e 15) increase sharply above 150 K and below 200 K (see below). Upon desorption of the multilayer (220 K), the positive-ion yields increase by more than 2 orders of magnitude, with the dominant signal at 93 amu, $OP(OCH_3)CH_3^+$ (Figure 3d). Other ions can, for the most part, be understood

(16) Holtzclaw, J. R.; Wyatt, J. R.; Campana, J. F. *Org. Mass Spectrosc.* **1985**, *20*, 90.
(17) Pritchard, J. G. *Org. Mass Spectrosc.* **1970**, *3*, 163.
(18) Meyerson, S.; Harvan, D. J.; Hass, J. R.; Ramirez, F.; Marecek, J. F. *J. Am. Chem. Soc.* **1984**, *106*, 6877.

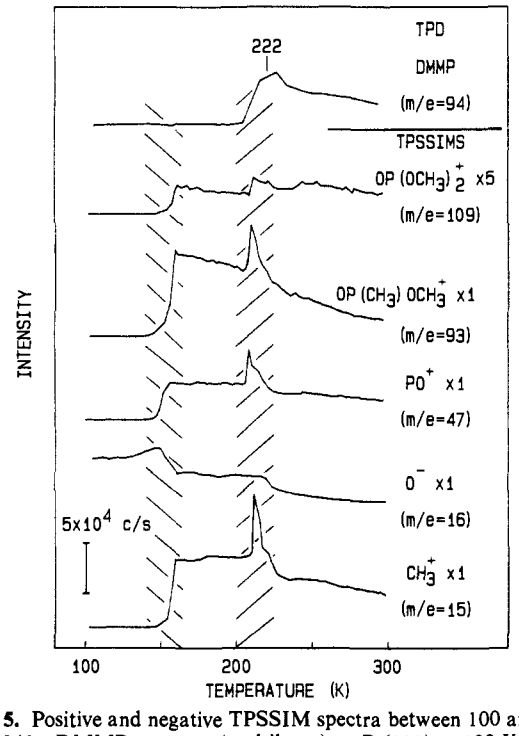

Figure 5. Positive and negative TPSSIM spectra between 100 and 300 K of a 240-s DMMP exposure (multilayer) on Pt(111) at 100 K. TPD spectrum of DMMP (m/e 94) from Figure 1 is included for comparison.

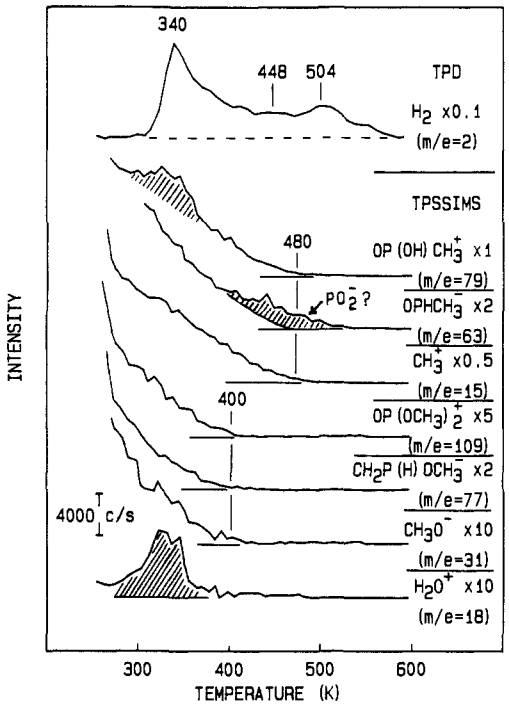

Figure 6. Positive and negative TPSSIM spectra between 250 and 600 K of a 240-s DMMP exposure on Pt(111) at 100 K. TPD spectrum of H_2 (m/e 2) from Figure 1 is included for comparison.

in terms of removing CH_3 and/or O fragments from the parent molecule (124 amu). The -SSIM spectrum of monolayer DMMP (Figure 4c) does not follow such a systematic pattern; the major ions are $OP(OCH_3)_2^-$ (m/e 109), PO_3^- (m/e 79), $CH_2P(H)OCH_3^-$ (m/e 77), $OP(H)CH_3^-/PO_2^-$ (m/e 63), OCH_3^-, OH^-, and O^-.

Above 350 K the ions containing OCH_3 groups [$OP(OCH_3)_2^{+/-}$ (m/e 109), $OP(OCH_3)CH_3^+$ (m/e 93), $CH_2P(H)OCH_3^{+/-}$ (m/e 77), OCH_3^-] attenuate to zero first, followed by those containing PCH_3 but no OCH_3 groups [$OP(OH)CH_3^+$ (m/e 79), $OP(H)CH_3^-$ (m/e 63), CH_3^+] and then those associated with PO_x species [PO_3^- (m/e 79), $P(OH)_2^+$ (m/e 65), $PO_2^{+/-}$ (m/e 63), and PO^+ (m/e 47)]. Although ions associated with m/e values greater than 120 could not be probed, the exclusion of polymeric species from our analysis is based on the absence of $P_2O^{+/-}$ (m/e 78), $P_2O_2^{+/-}$ (m/e 94), and $P_2O_3^{+/-}$ (m/e 110).

On the basis of SSIMS and TPD, we separate the thermal chemistry of DMMP on Pt(111) into three overlapping temperature regions: 100–300 K (Figure 5), 300–500 K (Figure 6), and 400–550 K (Figure 7). Figure 5 shows the positive- and negative-ion TPSSIM spectra from selected ions between 100 and 300 K resulting from a multilayer of DMMP. The DMMP (m/e 94) TPD spectrum of Figure 1 is included for comparison. The sharp ion yield changes mentioned previously are observed in the 140–175 and 200–235 K regions (highlighted in Figure 5). The latter region is coincident with desorption of multilayer DMMP (T_p = 222 K); however, there is no desorption in the 140–175 K region. The 140–175 K ion yield variations are not correlated with either the ion charge or the chemical type of ion. Among the negative ions, only the O^- and OH^- yields decreased. All of the positive ions increased.

DMMP decomposition on Pt(111) occurs in the second temperature range, 300–500 K. Figure 6 shows the H_2 TPD spectrum of Figure 1 and three types of SSIMS ions associated with DMMP decomposition. These three types involve OCH_3 groups (Figure 6b–d), CH_3 groups (Figure 6e–g), and OH groups (Figure 6a,g). The first set consists of ions with m/e values of +109, −77, and −31, which we assign to $OP(OCH_3)_2^+$, $CH_2P(H)OCH_3^-$, and OCH_3^-, respectively. These SSIMS ions reflect the stability of P–OCH_3 related species. They decay to zero by 450 K. Desorption of some H_2 and CO occurs in this same region (Figure 1). The second set of ions (Figure 6e–g) is characterized by m/e values of +79, −63, and +15 assigned to $OP(OH)CH_3^+$, $OP(H)CH_3^-$, and CH_3^+, respectively. All of these contain PCH_3 but not $POCH_3$. Except −63, which extends above 500 K (Figure 6f), these all go to zero near 500 K. The higher temperature tail of m/e −63 may be due to a small PO_2^- ion contribution from an unidentified PO_x species (to be discussed). The third set of ions involves OH-related species (Figure 6a,g). The H_2O^+ signal (Figure 6a) increases between 280 and 330 K and then decays sharply to zero at 350 K. The H_3O^+ signal (not shown), which is typically high when molecular H_2O is present,[19,20] has no in-

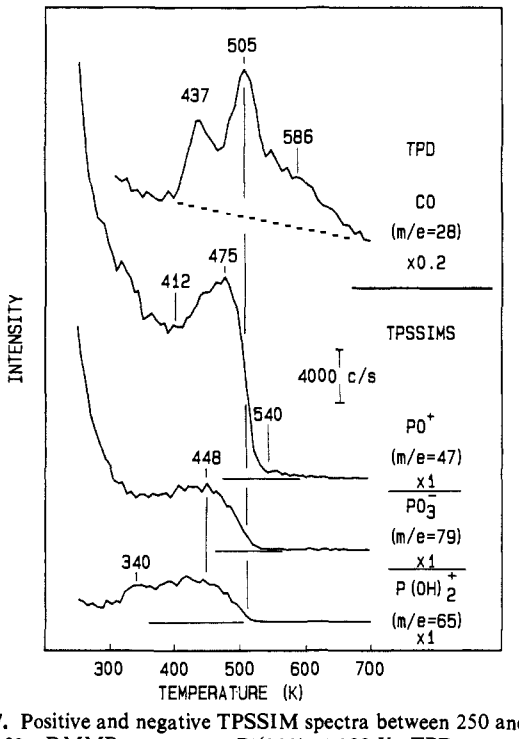

Figure 7. Positive and negative TPSSIM spectra between 250 and 700 K of a 150-s DMMP exposure on Pt(111) at 100 K. TPD spectrum of CO (m/e 28) from Figure 1 is included for comparison.

(19) Creighton, J. R.; White, J. M. *Surf. Sci.* **1982**, *122*, L648.

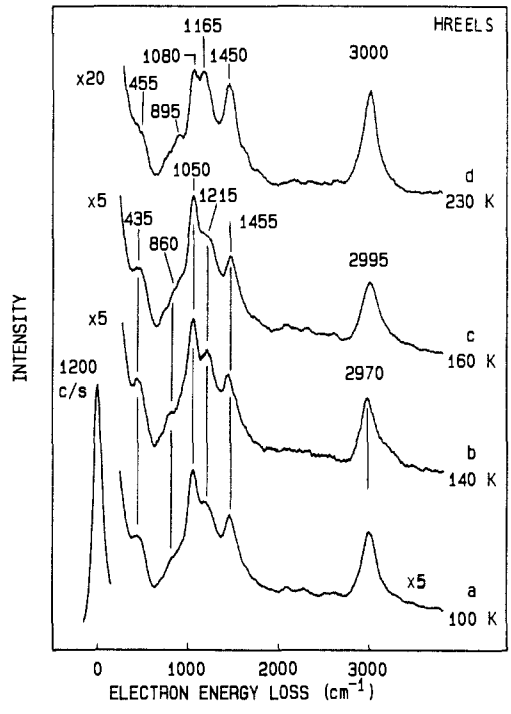

Figure 8. HREEL spectra of a 150-s DMMP exposure on Pt(111) (a) at 100 K, followed by heating to (b) 140 K, (c) 160 K, and (d) 230 K. The elastic peak count rate refers to the 100 K spectrum only.

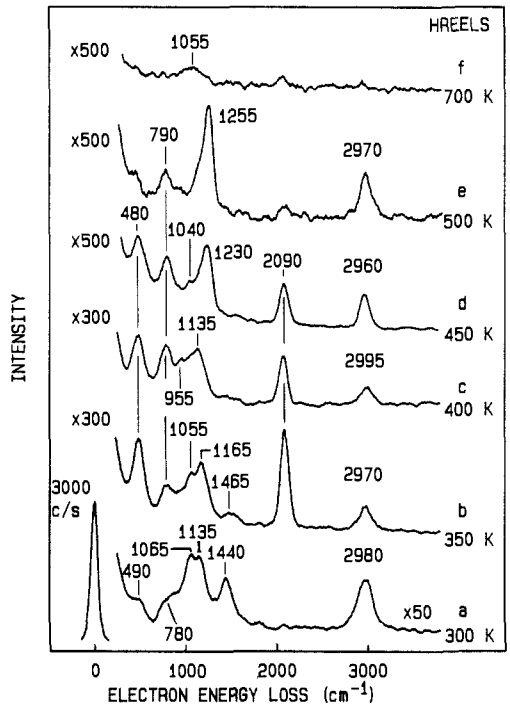

Figure 9. HREEL spectra of a 150-s DMMP exposure on Pt(111) at 100 K, followed by heating to (a) 300 K, (b) 350 K, (c) 400 K, (d) 450 K, (e) 500 K, and (f) 700 K. The elastic peak count rate refers to the 300 K spectrum only.

tensity from 100 to 600 K. The O^- and OH^- ion signals (also not shown) rise slightly at about 330 K and are only partially resolved from the signal decay associated with the parent molecule (Figure 4). The m/e +79 ($OP(OH)CH_3^+$) (Figure 6g) rises and falls with the other OH-related ions.

Figure 7 shows the last temperature region of interest (300–550 K). Changes in this region are attributed to decomposition of PO_x species. The TPSSIM spectra of PO_3^-, $P(OH)_2^+$, and PO^+ are shown with the CO TPD of Figure 1. The steep decays of the PO^+ and PO_3^- ions below 300 K are associated with multilayer DMMP desorption (Figure 5). The $P(OH)_2^+$ ion does not possess this background because it is not a major ion of molecular DMMP (Figure 3). The PO^+ signal rises between 410 and 475 K, and the $P(OH)_2^+$ and PO_3^- signals rise slightly above 300 K to maxima at about 450 K. The $P(OH)_2^+$ signal rise at 300 K is consistent with the OH-related ions. All three ions decay to zero coincident with the 505 K reaction limited CO TPD peak. The PO_3^- and $P(OH)_2^+$ ions are weaker than the PO^+ ion and start their decay about 30 K lower. PO^-, PO_3^+, and O^- do not track the signals of Figure 7, suggesting that they are not derived from PO_x species. The PO_2^- ion (Figure 6), as mentioned previously, and the PO_2^+ ion (not shown) do possess some intensity above 500 K ascribable to PO_x.

3.3. HREELS. The HREELS annealing set of multilayer DMMP on Pt(111) is shown in Figures 8 and 9. At 100 K, multilayer DMMP has losses at 2970, 1455, 1215, 1050, 860, and 435 cm^{-1}. These are assigned in Table I and compared to the IR[21] and Raman[13] spectra of liquid DMMP. In contrast to the obvious change in the SSIMS ion yields between 140 and 175 K (Figures 3–5), there is little difference between the HREEL spectra at 140 and 160 K (Figure 8b,c). The elastic peak count rate stays at approximately the same value as the 100 K spectrum (1200 counts/s). After heating to 160 K, the loss at 2970 cm^{-1} (140 K) shifts to 2995 cm^{-1}, and the 860- and 1215-cm^{-1} loss regions broaden. The HREELS spectrum changes slightly by heating to just above the DMMP multilayer desorption temperature, 230 K (Figure 8d). The elastic peak count rate approximately doubles (2200 counts/s). The 1215- and 1050-cm^{-1} losses shift to 1165 and 1080 cm^{-1}, respectively, and the relative intensity of the latter decreases. There are no major changese compared to multilayer DMMP, and there are no losses due to species such as CO, H_2O, C_xH, or O.

Table I. HREEL Frequencies (cm^{-1}) of Multilayer (100 K) DMMP on Pt(111)[a] and IR[b] and Raman[c] Frequencies of Liquid DMMP

	multilayer DMMP on Pt(111), 100 K	liquid DMMP	
		IR	Raman
$\nu_a(OCH_3)$	2970	3000	3022
$\nu_a(PCH_3)$		2960	2999
$\nu_s(OCH_3)$		2935	2957/2852
$\nu_s(PCH_3)$		2865	2928
$\delta_a(OCH_3)$	1455	1512	1466/1454
$\delta_a(PCH_3)$		1465	
$\delta_s(OCH_3)$		1422	1421
$\delta_s(PCH_3)$		1315	1313
ν(P=O)	1215	1246	1240
ν(PO—C)	1050	1060/1035	1058/1032
$\rho((O)CH_3)$		1186	1186/1032
$\rho((P)CH_3)$	860	915/820	896
ν(P—OC)	nr	788	820/788
ν(PC)	nr	714	714/705
δ_a(POC)	435		
δ_s(POC)			502
$\delta_a(OPO_2)$			467
$\delta_s(OPO_2)$			414
$\delta_a(PO_2)$	nr		306
$\delta_s(PO_2)$	nr		

[a] This work. [b] Reference 21. [c] Reference 13. [d] Key: ν = stretch, δ = deformation, ρ = rock, a = asymmetric, s = symmetric, nr = not resolved.

A small amount of DMMP decomposition occurs after heating to 300 K (Figure 9a). Very weak CO losses appear at 2080 and 1795 cm^{-1}, and the 780-cm^{-1} shoulder becomes more pronounced. Substantial decomposition occurs after heating to 350 K (Figure 9b), and the elastic peak count rate increases with 3.0×10^3 counts/s at 300 K to 2.5×10^4 counts/s at 350 K. The dominant losses are now due to atop CO at 2090 (ν(CO)) and 480 cm^{-1} (ν(PtC)). The 1465- and 1055-cm^{-1} losses are weaker, and the 790-cm^{-1} loss is now resolvable. As expected from TPD of CO, heating to 400 K decreases the 2080-cm^{-1} intensity (Figure 9d). The 1465- and 1055-cm^{-1} losses are almost gone, leaving a broad

(20) Ogle, K. M.; White, J. M. *Surf. Sci.* **1986**, *425*, 425.
(21) Guilbault, G. G.; Scheide, E.; Das, J. *Spectrosc. Lett.* **1968**, *1*, 167.

set of bands between 900 and 1150 cm^{-1}. The 790-cm^{-1} loss increases, and the 1135-cm^{-1} loss retains significnat intensity. Heating to 450 K (Figure 9d) shifts the latter to 1230 cm^{-1}, leaving a weak loss at 1040 cm^{-1}. After heating to 500 K, the 1230-cm^{-1} loss shifts to 1255 cm^{-1} and strengthens. The remaining losses are at 2970 and 790 cm^{-1}. The elastic peak count rate also increases by a factor of 3 from the 450 K spectrum (3.6×10^4 to 1.3×10^5 counts/s). Heating to 700 K decreases the count rate to 2.8×10^4 counts/s and leaves a very weak and broad loss at 1055 cm^{-1}, a small signal at 2030 cm^{-1} due to background CO adsorption, and a tiny signal in the C–H stretching region, 2940 cm^{-1}.

4. Discussion

4.1. Multilayer DMMP, 100–200 K. Table I compares the HREELS assignments of multilayer DMMP on Pt(111) with the IR[22] and Raman[13] frequencies of liquid DMMP. The assignments generally agree, particularly considering the lower resolution of HREELS. For DMMP, and molecules like it, the ν(P=O) mode is very sensitive to the structural conformation of the molecule, which partially depends upon the solvent environment.[23,24] The more polar the environment, the lower the ν(P=O) frequency. The varied polarity of the molecule is largely the result of hindered rotation about the P–OCH_3 bonds.[25] The gas-phase monomer has a ν(P=O) frequency of 1260 cm^{-1}, while the ν(P=O) of solid DMMP is at 1202 cm^{-1}.[23] Barnes and co-workers[23] have also shown that the ν(P=O) of DMMP monomers imbedded in an inert matrix shift by about 20 cm^{-1} from the gas-phase frequency (1260 cm^{-1}), while aggregate formation in the matrix results in 40-cm^{-1} shifts. The ν(P=O) loss for multilayer DMMP on Pt(111) (Figure 8a) is at 1215 cm^{-1}, suggesting that the conformation in the ice is very polar. This agrees with the results of Barnes et al. and with work function measurements of Hegde et al. for multilayer DMMP on Rh(100) at 100 K.[4]

Major SSIMS yield changes occur for the multilayer between 140 and 175 K (Figures 3–5), but there are no strong changes in HREELS (Figure 8b,c). These SSIMS yield changes could result from (1) reaction within the multilayer, (2) desorption of a species other than DMMP trapped in the multilayer, and/or (3) a restructuring of the multilayer. Since there are no TPD products in this thermal region, since HREELS does not indicate the devleopment new loss features, and since there are SSIMS ion signals from H_2O, a common impurity known to react with phosphorus esters to form alcohols and acids, we discount the first two.

Detection of subtle structural changes, if they occur, by HREELS would be limited by the low resolution of the spectrometer (80–100 cm^{-1}). Most, but not all, of the positive- and negative-ion yields increase in intensity between 140 and 175 K. This eliminates work function changes as the sole cause. We propose that these ion yield changes result from a restructuring of the multilayer, leaving it more polar and more densely packed. Changing the polarity should alter the yields, and the higher density should increase the Ar^+–DMMP collision cross section and thus all the ion yields. Both possibilities can be interpreted either intra- or intermolecularly.

4.2. Monolayer DMMP. Turning from multilayer to monolayer DMMP, we note that, as for Rh(100),[4] DMMP is anchored to the Pt(111) surface through the oxygen end of the –P=O group since the ν(P=O) loss shifts from 1215 cm^{-1} for the multilayer of 1165 cm^{-1} for the adsorbed layer (Figure 8d). Similar red shifts have been observed by Templeton and Weinberg for DMMP on Al_2O_3,[9] by Guilbault et al. for DMMP on $FeCl_3$[21] and $CuCl_2$,[26] and for numerous monodentate DMMP–metal complexes.[27–32]

Table II. HREEL Frequencies (cm^{-1}) of Monolayer DMMP (230 K) on Pt(111),[a] IETS Frequencies of DMMP on Al_2O_3,[b] IR Frequencies of DMMP on $FeCl_3$,[c] and HREEL Frequencies of Monolayer CH_3OH on Pt(111)[d]

	Pt(111), 230 K	Al_2O_3, 200 K	$FeCl_3$, 300 K	CH_3OH/Pt(111), 150 K	
$\nu_a(OCH_3)$	3000	2981			
$\nu_a(PCH_3)$					
$\nu_s(OCH_3)$		2843	2961	2930	$\nu_s(OCH_3)$
$\nu_s(PCH_3)$		2912	2856		
$\delta_a(OCH_3)$	1450	1452			
$\delta_a(PCH_3)$		1409			
$\delta_s(OCH_3)$			1314	1430	$\delta_s(OCH_3)$
$\delta_s(PCH_3)$		1308			
ν(P=O)	1165		1173		
ν(PO–C)	1080	1048	1052/1021	1000	ν(O–C)
$\rho((O)CH_3)$	nr	1177/1166			$\rho((O)CH_3)$
$\rho((P)CH_3)$	895	900	915/828		
ν(P–OC)	790, nr	830	795		
ν(PC)	nr	736/721			
δ_a(POC)	455	501			
δ_s(POC)		469			
$\delta_a(OPO_2)$		413			
$\delta_s(OPO_2)$		310			
$\delta_a(PO_2)$	nr				
$\delta_s(PO_2)$	nr				
ν(Pt–O)	nr				

[a] This work. [b] Reference 13. [c] Reference 21. [d] Reference 33.

Chart II

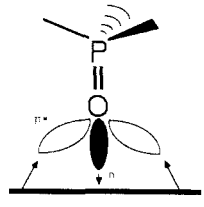

Chart III

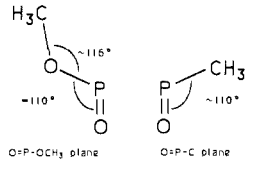

Table II compares the HREELS losses of monolayer DMMP on Pt(111) (Figure 8d) with earlier work.[13,21] The HREELS frequencies of methanol on Pt(111)[33] at 150 K are also included. Compared to liquid DMMP (Table I), the major change in three DMMP systems is in the red-shifted ν(P=O) mode, which corresponds to a weakening of the P=O bond due to chemisorption. This involves σ donation to the metal from the O lone pairs and possible back-bonding of the filled metal orbitals into the P=O π-antibonding orbital according to Chart II.

The ν(Pt–O) loss for DMMP adsorbed according to Chart II is absent from Figure 8d, probably because it cannot be resolved from the wings of the elastic peak. We expect it to lie below 350 cm^{-1} on the basis of data for $[M(DMMP)_x](ClO_4)_y$ complexes.[27] Chart II also accounts for the unchanged frequencies for the other modes of DMMP (see Table II and Figure 8). An exception is the ν(PO–C) loss, which *increases* by 30 cm^{-1}. Similar shifts have

(22) Burkhardt, V. W. D.; Höhn, E.-G.; Goubeau, J. *Z. Anorg. Allg. Chem.* **1978**, *442*, 19.
(23) Barnes, A. J.; Lomax, S.; Van der Veken, B. J. *J. Mol. Struct.* **1983**, *99*, 137.
(24) Van der Veken, B. J.; Herman, M. A.; Barnes, A. J. *J. Mol. Struct.* **1983**, *99*, 197.
(25) Van der Veken, B. J.; Herman, M. A. *J. Mol. Struct.* **1977**, *42*, 161.
(26) Scheide, E. P.; Guilbault, G. G. *J. Inorg. Nucl. Chem.* **1971**, *33*, 1689.
(27) Karayannis, N. M.; Mikulski, C. M.; Strocko, M. J.; Pytlewski, L. L.; Labes, M. M. *Inorg. Chim. Acta* **1974**, *8*, 91.
(28) Pudovik, A. N.; Muratova, A. A.; Yarkova, E. G.; Marsheva, V. N. *J. Gen. Chem. USSR* **1968**, *38*, 2439.
(29) Karayannis, N. M.; Owens, C.; Pytlewski, L. L.; Labes, M. M. *J. Inorg. Nucl. Chem.* **1969**, *31*, 2059 and 2767.
(30) Frankel, L. S. *Inorg. Chem.* **1969**, *8*, 1784.
(31) Karyannis, N. M.; Mikulski, C. M.; Gelfand, L. S.; Pytlewski, L. L. *J. Inorg. Nucl. Chem.* **1978**, *40*, 1513.
(32) Cohen, C. S.; Smith, J. D. *J. Chem. Soc. A* **1969**, 2087.
(33) Sexton, B. A. *Surf. Sci.* **1981**, *102*, 271.

Chart IV

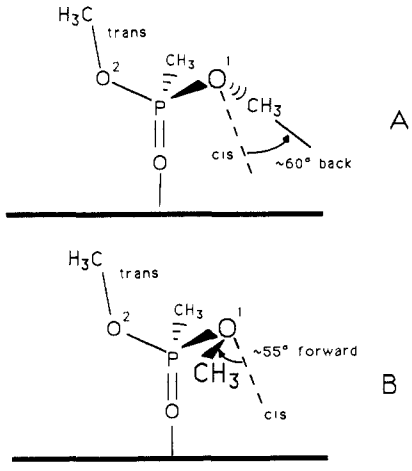

(Dashed lines are in the plane of the O=P-O^1 bonds)

Chart V

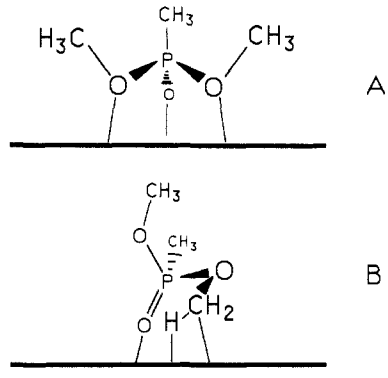

been observed by IR for DMMP complexes[28] and for several other phosphonate ester complexes[32] chelated through the -P=O oxygen lone pairs. The increased ν(PO-C) frequency also implies that DMMP is not coordinated to Pt through the methoxy O lone pairs.

The relatively low intensity of the ν(P-C) and ν(P-OC) losses is interesting. For trimethylphosphine ($P(CH_3)_3$) adsorbed on Pt(111), the ν_s(P-C) HREELS loss is very intense compared to the CH_3-related losses.[6] The weakness of these modes is likely due to the orientations of the P-C and P-OC bonds with respect to the surface. Assuming that DMMP is bound through the P=O oxygen atom and that the P=O axis is normal to the surface, the P-CH_3 and P-OCH_3 bond axes will have significant components parallel to the surface (Chart III). If this picture is appropriate, the low intensity is ascribable to image dipole effects and the dipole selection rule.

DMMP has a number of possible metastable conformers. The most stable ones for isolated DMMP are aligned to minimize the methyl steric interactions. According to Van der Veken and Herman,[25] these conformations would place one methoxy group relatively normal to the surface and trans with respect to the P=O bond (Chart IVA,B). The other methoxy group would be rotated roughly 50–60° in either direction from the cis position. Both configurations have dipole moments greater than 5.3 D (debye) in the gas phase. The most polar configuration of DMMP (7.5 D), in which both methoxy groups are trans and rotated between 150° and 190° from the -P=O group, is not as stable as those of Chart IV.

4.3. DMMP Decomposition. Because the most obvious decomposition product, CO, is absent and because all the other HREELS bands are ascribable to adsorbed DMMP, we conclude that adsorbed DMMP does not decompose on Pt(111) below 300 K. The lack of any desorption below 300 K, other than multilayer DMMP, also supports molecular adsorption.

At higher temperatures, approximately 0.09 ML of DMMP decomposes during TPD of a multilayer dosed at 100 K (Figure 1). Estimating the volume occupied by one DMMP molecule from the liquid density and molecular weight, we calculate a molecular van der Waals radius of 3.5 Å and a maximum coverage of about 0.15 ML. Assuming the bonding geometry of Chart III and using bond lengths and angles,[25] we estimate an average molecular van der Waals radius parallel to the surface of about 3.4 ± 0.4 Å. A projected circle of this radius upon the Pt(111) surface overlaps 8.5 ± 2 Pt atoms, corresponding to a coverage of 0.12 ± 0.3 mL, in reasonable agreement with the above estimate. These two estimates allow for significant molecular DMMP desorption (up to 0.06 ML) from the first layer as observed on Rh(100).[4]

As the temperature increases, the decomposition of DMMP proceeds qualitatively in the following steps: (1) PO-C bond cleavage and some P-OC bond cleavage (300–450 K), (2) P-C bond cleavage (400–500 K), and (3) PO_x decomposition (450–550 K). These will be discussed in order below.

4.3.1. PO-C and P-OC Bond Cleavages. Above 300 K, DMMP decomposition yields HREELS losses assignable to adsorbed CO (2090, 1810, 480 cm^{-1}) and CH (790 cm^{-1}) (Figure 9b). Intensity decreases in the $\delta(CH_3)$ (1465 cm^{-1}), ν(P=O) (1165 cm^{-1}) and ν(C—O) (1055 cm^{-1}) losses of DMMP, as well as an 8-fold increase in the elastic peak count rate, also indicate decomposition. The mechanism is undoubtedly complex. TPSSIMS results (Figure 6) indicate that the first step involves methoxy decomposition as the $OP(OCH_3)_2^+$, $CH_2P(H)OCH_3^-$, and OCH_3^- ion intensities all decay to zero before 400 K. This process is accompanied by H_2 TPD peaking at 340 K.

Three important observations about the methoxy decomposition between 300 and 450 K are obtained from TPD (Figures 1 and 2).

(1) At monolayer saturation, over half of the total H_2 desorbs between 300 and 450 K, and some of it is reaction-limited. This H_2 results mainly from CH bond cleavage in the $POCH_3$ groups.

(2) At monolayer saturation, 20% (about 0.054 ML) of the evolved CO is desorption limited (T_p = 437 K). This CO results from $POCH_3$ decomposition to CO and three H, as in the case of CH_3OH decomposition on Pt(111).[33] The remaining 80% (or about 0.216 ML) results from the decomposition and reaction of other C- and O-containing species above 450 K. Since 67% (0.18 ML) of the available O in the parent molecule exists as $-OCH_3$ groups, the desorption-limited CO must result from P-OC bond cleavage in at least 30% (0.054/0.18) of the $POCH_3$ groups. The remaining $POCH_3$ groups (70%) decompose by O-C bond cleavage to CH and two H, leaving the P-O bond intact.

For low coverages, there is no desorption-limited CO. We interpret this as indicating a much higher probability of PO-CH_3 bond cleavage than at high coverages and suggesting that steric interactions in the compressed overlayer enhance P-OCH_3 bond cleavage.

At low coverages, Chart VA is a likely intermediate in the first step of DMMP decomposition. HREELS and SSIMS results suggest that the majority of the P-O bonds are still intact above 400 K (to be discussed). At monolayer saturation, the steric constraints may limit the extent to which both methoxy oxygens of DMMP interact with the surface. Alternatively, the methoxy that is rotationally trapped in the conformation of Chart IVB may first decompose by C-H bond cleavage to a formaldehyde-like intermediate (Chart VB), which then decomposes to CO, H, and phosphorus species. Formaldehyde by itself on Pt(111) readily decomposes to CO and H at 300 K.[34,35]

(3) The third significant TPD result is that CH_4, H_2O, CH_3OH, and CO_2 are not observed in TPD. The absence of H_2O and CO_2 suggests that atomic O, which is very reactive on Pt(111) in the presence of H or CO, is not a product of PO-C or P-OC bond cleavage, at least below 450 K where surface H and CO are available. The absence of CH_4 and CH_3OH suggests that deh-

(34) Abbas, N. M.; Madix, R. J. *Appl. Surf. Sci.* **1981**, *7*, 241.
(35) Henderson, M. A.; Mitchell, G. E.; White, J. M. *Surf. Sci.* **1987**, *188*, 206.

Scheme I

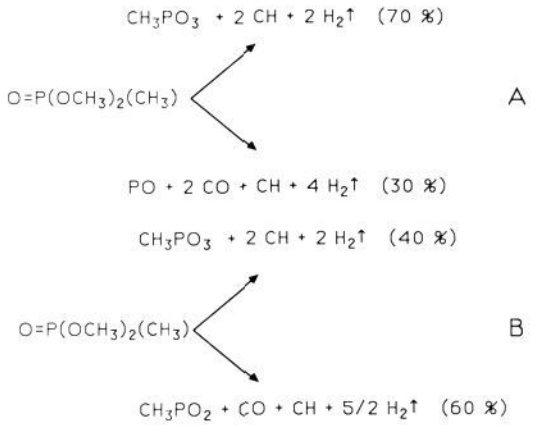

Chart VI

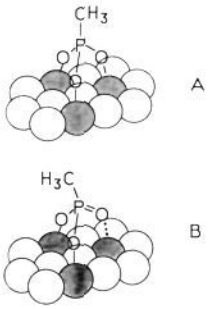

ydrogenation completely dominates hydrogenation as in CH_3OH decomposition on Pt(111).[33] The presence of OH-related SSIMS ion signals between 300 and 350 K suggests either that surface H participates in PO–C bond cleavage by reacting with the O or, less likely, that the $OH^{+/-}$ and H_2O^+ signals are formed during the SSIMS process.

At 400 K, most of the surface species have a P–CH_3 bond and multiple P–O bonds. We propose two reaction schemes (Scheme I) for the initial DMMP decomposition process. Both are based on the formation of 0.054 ML of desorption limited CO. In A, 70% of the DMMP decomposes with no P—O bond cleavage to a CH_3PO_3 species and 30% decomposes to P═O and 0.054 ML of CO. In B, 40% decomposes to CH_3PO_3 and 60% has one P–O bond cleaved, resulting in a CH_3PO_2 species and 0.054 ML CO. Both mechanisms account for the 0.054-ML desorption-limited CO and the absence of atomic O and significant amounts of P═O below 400 K (to be discussed). The amounts of desorption-limited H calculated from A and B are 0.46 and 0.36 ML, respectively, indicating that if B is operative, some of the measured 0.42 ML of H may result from P–CH_3 decomposition (to be discussed).

The stability of the proposed CH_3PO_3 and CH_3PO_2 species on Pt(111) cannot be directly addressed, although it is clear that the CH_3-related SSIMS ions (Figure 6) and the $\delta(CH_3)$ HREELS loss at 1465 cm^{-1} (Figure 9b) attenuate above 400 K and before desorption of reaction-limited CO (505 K). Structurally, mechanism A is favored for reasons indicated below. Two reasonable structures of a CH_3PO_3 species are shown in Chart VI.

The first structure (**1**) is roughly C_{3v} and should have strong HREELS losses for $\nu_s(PO_3)$ and ν(PC) modes. Typical $\nu_s(PO_3)$ frequencies for solid RPO_3^{2-} salts vary between 960 and 1000 cm^{-1}.[36-38] Templeton and Weinberg[13] proposed CH_3PO_3 as an intermediate in DMMP and methylphosphonic acid (MPA) decomposition on Al_2O_3 and assigned a 1035-cm^{-1} peak to $\nu_s(PO_3)$. However, Higo et al.[39] assigned a 900-cm^{-1} IR peak to the $\nu_s(PO_3)$ mode of decomposed MPA on Al_2O_3. Dines and DiGiacomo[40] have attributed at 1045-cm^{-1} IR peak to the $\nu_s(PO_3)$ mode of crystalline $Zr(O_3PR)_2$. Structure **1** could then be responsible for the 955-cm^{-1} loss ($\nu_s(PO_3)$) observed in HREELS after heating DMMP to 350 K (Figure 9b). The second structure (**2**) has C_s symmetry, and the P═O bond is weakly coordinated to the surface. The ν(P═O) stretch of **2** should resemble that of O═$P(CH_3)(OH)_2$ at 1140 cm^{-1}.[38] This is consistent with the 1135-cm^{-1} HREELS loss (ν(P═O)) in Figure 8c. The ν(PC) loss of either species is probably obscured by the δ(CH) mode of CH at 790 cm^{-1}.

Chart VII

If formed, CH_3PO_2 (mechanism B) would probably involve either η^1 (O) or η^2 (O, O) bonding. However, there is no evidence for either in the inorganic literature. Thus, B is not favored.

4.3.2. P–CH_3 Bond Cleavage, 400–500 K. TPSSIMS suggests that P–CH_3 bonds break at higher temperatures than PO–CH_3 bonds (Figure 5). Ions associated with the PCH_3 group ($OP(OH)CH_3^+$ (m/e 79), $OP(H)CH_3^-$ (m/e 63), and CH_3^+) attenuate to zero between 450 and 500 K, coincident with the poorly resolved H_2 TPD state at 450 K (Figure 6). Although the m/e values of +79 and −63 might be PO_3^+ and PO_2^-, respectively, their signals do not track the PO_x ions of Figure 7. Thus, we assign them to $OP(OH)CH_3^+$ and $OP(H)CH_3^-$, respectively.

Based on this SSIMS evidence, we propose that PCH_3 decomposes by

$$CH_3PO_3 \xrightarrow{400\text{–}500\ K} PO + CH + H_2 + 2O \qquad (2)$$

The rise in the PO^+ signal (Figure 7) at 400 K is consistent with the formation of PO in this step. As for low coverages of $P(CH_3)_3$,[6] methane is not observed in this decomposition because the coverage of PCH_3 groups is too low (less than 0.09 ML).

The decomposition of CH_3PO_3 is accompanied by a decrease in the HREELS intensity between 900 and 1050 cm^{-1} and a shift of ν(P═O) from 1135 to 1255 cm^{-1} (Figure 9e). The loss at 480 cm^{-1} in Figure 9c,d is assigned to a combination of the ν(Pt–O) loss of atomic O[41] and ν(Pt–C) of CO. The weak 1040-cm^{-1} loss is probably from undecomposed CH_3PO_3 or an unidentified PO_x species.

4.3.3. PO_x Decomposition, 450–550 K. The only species remaining on the surface above 500 K are CH (2970, 790 cm^{-1}), atomic O, and PO_x. HREELS and SSIMS suggest that two PO_x species are present. PO is dominant (Chart VII) and gives a strong PO^+ (m/e 47) SSIMS signal and a ν(P═O) loss at 1255 cm^{-1} (Figure 9e). Absence of intense ν(P–O) losses below 1100 cm^{-1} suggests that the P to O ratio is 1:1. When PO decomposes, there is a sharp drop in the PO^+ SSIMS signal and CO desorption (from C + O) at 505 K. Assuming CO desorption is limited by P═O bond breaking, a Redhead analysis[42] of the 505 K CO peak yields an activation barrier for P–O decomposition of 30.3 kcal/mol. A second estimate comes from analysis of the PO^+ TPSSIMS decay. This approach yields an activation barrier of 35.9 kcal/mol and a preexponential of 2×10^{15} s^{-1}.[43] Decomposition of the unidentified PO_x species begins at 450 K (Figure 7a,b), about 30 K prior to PO decomposition. However, the PO_3^-, $P(OH)_2^+$, and PO^+ ions all attenuate to zero near 520 K. The additional CO desorption above 520 K is from residual C + O, and not from decomposition of another phosphorus-related species.

4.4. Implications for Catalytic Oxidation. A major problem in catalytic oxidation of organophosphorus compounds is deac-

(36) Corbridge, D. E. C.; Lowe, E. J. *J. Chem. Soc.* **1954**, 4555.
(37) Tsuboi, M. *J. Am. Chem. Soc.* **1957**, *79*, 1351.
(38) Van der Veken, B. J.; Herman, M. A. *J. Mol. Struct.* **1973**, *15*, 225.
(39) Higo, M.; Owaki, Y.; Kamata S. *Chem. Lett.* **1985**, 1309.
(40) Dines, M. B.; DiGiacomo, P. M. *Inorg. Chem.* **1981**, *20*, 92.
(41) Gland, J. L.; Sexton, B. A.; Fisher, G. B. *Surf. Sci.* **1980**, *95*, 587.
(42) Redhead, P. *Vacuum* **1962**, *12*, 203.
(43) Ogle, K. M.; Creighton, J. R.; Akhter, S.; White, J. M. *Surf. Sci.* **1986**, *169*, 246.

tivation due to accumulation of P on the catalyst. For example, P from decomposed PH_3 diffuses in and out of Pt(111) above 300 K and is very difficult to remove by oxidation, espeically at high coverages.[7] The key to these oxidative processes is the removal of P by PO_x formation and desorption *before* atomic P forms.

In a recent study by Smentkowski et al.[10] *catalytic* decomposition of DMMP was observed on Mo(110) above 898 K in a 2:1 O_2–DMMP molecular beam without accumulation of P or C on the surface. The Mo(110) surface formed a stable oxide layer that catalyzed DMMP decomposition but prevented accumulation and bulk diffusion of P. Our results for DMMP decomposition on α-Fe_2O_3[9] show that it is active for DMMP decomposition but deactivates as phosphate forms.

Unlike Mo, Pt does not readily form a stable bulk oxide. Thus, removal of P can occur only when gas-phase oxygen is present to drive the formation of PO_x. In the absence of O_2, these PO_x species are stable only below 500 K. The dominant PO_x species observed in this study is PO. In the absence of O, it decomposes with an activation barrier of 35.9 kcal/mol, about 23 kcal/mol lower than its desorption barrier from Pt.[11] Thus removal of PO in a catalytic process of Pt will require high temperature to overcome the desorption barrier and high pressures of O_2 to maintain P–O bonds. Our results suggest that, in the absence of O_2, DMMP decomposition on Pt(111) above 600 K will lead to phosphorus accumulation and catalytic deactivation.

5. Summary

(1) At 100 K on Pt(111), DMMP adsorbs molecularly through the oxygen lone pairs of the –P=O group. This structure is stable to 300 K.

(2) TPD after a multilayer exposure of DMMP at 100 K gives multilayer desorption (220 K) and 0.09 ML of DMMP decomposition. The products are 0.27 ML of CO (437, 505, 586 K), 0.79 ML of H_2 (340, 448, 504 K), surface P, and a small amount of surface C.

(3) TPSSIMS results indicate that, between 300 and 500 K, DMMP decomposes in steps to PO_x. Near 300 K PO–C bonds cleave, with some P–OC bond cleavage at high-DMMP coverages. At higher temperatures, P–C bonds cleave, leaving at least two PO_x species on the surface.

(4) The dominant PO_x species is PO, which is characterized by a 1255-cm^{-1} ν(P=O) loss in HREELS and an intense PO^+ SSIMS signal. It is stable to at least 500 K.

Acknowledgment. This research was supported in part by the U.S. Army Research Office. We gratefully acknowledge helpful discussions with Dr. Rama Hegde.

Registry No. Pt, 7440-06-4; DMMP, 756-79-6.

Molecular Orbital Approach to Substituent Effects in Amine–CO_2 Interactions

A. K. Chakraborty, K. B. Bischoff,* G. Astarita, and J. R. Damewood, Jr.

Contribution from the Departments of Chemical Engineering and Chemistry and The Center for Catalytic Science and Technology, University of Delaware, Newark, Delaware 19716.
Received April 3, 1987

Abstract: The effects of substituents at the α-carbon atom on the donor properties of primary amines and amino alcohols have been studied. Such substituted amino species have important applications in industrially relevant gas-separation processes. Qualitative molecular orbital arguments, along with detailed calculations at the MNDO level of theory, show that upon methyl substitution at the α-carbon atom the interactions of the methyl group orbitals with the nitrogen lone-pair orbital lead to subtle but significant changes in the donor properties of the amino species. Infrared spectroscopic data supporting the calculations are also described. The implications of changes in the donor properties of the amino species on its reactions with acidic gases, such as CO_2, have been considered. These studies serve to elucidate previous phenomenological results regarding the macroscopic kinetic and equilibrium behavior of substituted amino species in CO_2 absorption applications.

1. Introduction

The removal of acidic gases such as CO_2, H_2S, and SO_2 from gas streams is widespread in the chemical processing industries.[1] This separation is commonly accomplished by absorbing the acidic gas into a chemically reactive liquid. Carrying out such processes efficiently is of crucial importance from several viewpoints, and a detailed understanding of these reacting, two-phase systems is therefore necessary.

The absorption of an acidic gas into a chemically reacting liquid is a mass-transfer process accompanied by a Lewis acid–base reaction. There are therefore two aspects of the problem that need consideration. On one hand, the facilitated-transport problem of mass transfer with chemical reaction needs to be understood within the framework of macroscopic phenomenological models. On the other hand, a comprehensive understanding of the system is possible only if the fundamental molecular chemistry and its macroscopic manifestations are clearly elucidated. Such an understanding is crucial if one is to attain the goal of being able to "tailor-make" molecules that could carry out chemical absorption based separations in a very specific manner.

While the literature (particularly in engineering science) is rich with work on the facilitated-transport problem,[2-5] relatively little emphasis has been placed on a fundamental understanding of the molecular chemistry of these systems. In this paper, the reactions of a model acidic gas (CO_2) with various amines and amino alcohols are investigated. In particular, the effects of substituents on the Lewis acid–base interaction is investigated within the theoretical framework of perturbation molecular orbital theory[6]

(1) Charpentier, J. C. *Chem. Eng. Res. Des.* **1982**, *60*, 131.

(2) Astarita, G.; Bisio, A.; Savage, D. W. *Gas Treating With Chemical Solvents*; Wiley-Interscience: New York, 1983.

(3) Danckwerts, P. V. *Gas-Liquid Reactions*; McGraw-Hill: New York, 1970.

(4) Astarita, G.; Savage, D. W. *Chem. Eng. Sci.* **1980**, *35*, 659.

(5) Danckwerts, P. V.; Sharma, M. M. *Chem. Eng. (N.Y.)* **1966**, 244.

(6) Fukui, K. In *Molecular Orbitals in Physics, Chemistry and Biology*; Lowdin, P. O., Pullman, B., Eds.; Academic: New York, 1964.

0002-7863/88/1510-6947$01.50/0